DE-COHERENCE EFFECTS IN UNDERWATER ACOUSTCS: SCALED EXPERIMENTS.

Gaultier Real[a,b], Jean-Pierre Sessarego[a], Xavier Cristol [b] and Dominique Fattaccioli[c]

[a]Laboratoire de Mécanique et d'Acoustique (LMA), CNRS, 31 Chemin Joseph Aiguier, 13402 Marseille cedex 20, France.
[b]Thales Underwater Systems SAS, 525 route des Dolines, 06903 Sophia-Antipolis, France.
[c]Direction Générale de l'Armement – DGA Techniques navales, avenue de la Tour Royale, BP 40915, 83050 Toulon Cedex, France.

Contact author: Real Gaultier: real@lma.cnrs-mrs.fr

Abstract**:** *We reproduce, using scaled experiments in a water tank, the effects of scattering phenomena responsible for the degradations of sonar system performances in oceanic environment (typically, the small sound speed fluctuations associated with linear internal waves). We reproduce a wide panel of scattering effects, spanning from "simple" phase aberrations up to radical changes in the sound field structure (appearance of caustics).*
An experimental protocol was developed. It consists in transmitting a high-frequency wave train (ultrasonic pressure field around 2MHz) through wax lenses with randomly rough faces, that induce distortions comparable to those that would be observed at sea at around 1kHz in the case of a lower frequency acoustic signal travelling through a linear internal wave field. Using a 3-D printer, we were able to manufacture lenses with a randomly rough face characterized by its amplitude and vertical and horizontal correlation lengths.
The dependence of the various parameters involved in the experiment (related to the object, distance of propagation, frequency, …) were studied using simulation programs allowing to measure the average number of eigen rays and the phase difference between the extreme micro paths. Those two quantities are useful to compare our results to what was obtained in the literature, in particular to Flatté's dimensionless analysis.
The propagation through the lenses was then studied in a water tank using virtual arrays (automatic displacements of a hydrophone). We represent the results using the acoustic envelop in order to observe wave front distortions or appearance of caustics.
Measurements of the coherence function and, hence, of the radius of coherence, are carried out. Finally, we observe degradation of the performances of a localization algorithm.

Keywords: *De-coherence, Tank Experiments, Fluctuations, Dimensionless Analysis.*

1. INTRODUCTION.

We focus here on the topic of wave propagation in random media (WPRM). Even though a considerable amount of contributions to the field is available in the literature ([1-5]), our thought is that providing experimental data acquired in controlled environment would be of great help in order to understand the involved physical phenomena. Our main objective is therefore to develop an experimental protocol allowing us to measure in a water tank (i.e. at reduced scale) signal distortions comparable to what would be observed in the case of a lower frequency sound wave traveling through a spatially fluctuating ocean. As an example, linear internal waves (LIW) are responsible for perturbations in the underwater sound propagation, and induce some degradation of the array performances [6-9].

The objective of this research, in fine, is to provide some corrective signal processing techniques in order to compensate for these de-coherence effects [10].

2. SIMULATION STUDY.

In order to anticipate for the induced distortion of the acoustic signals, we developed a ray tracing program allowing us to calculate the average number of eigen rays $\langle N_{eig} \rangle$ and the rms phase difference between the extreme micropaths $\Delta_{\varphi RMS}$. According to Flatté [5], these two quantites are related to the dimensionless parameters Λ (diffraction parameter) and Φ (strength parameter) used to classify the signal fluctuations. The relationships between the quantities previously cited have been verified in [11]. Hence, tracing rays through a specific wax lens allows us to anticipate for the fluctuation regimes involved in a given experimental configuration, as depicted by Fig.1.

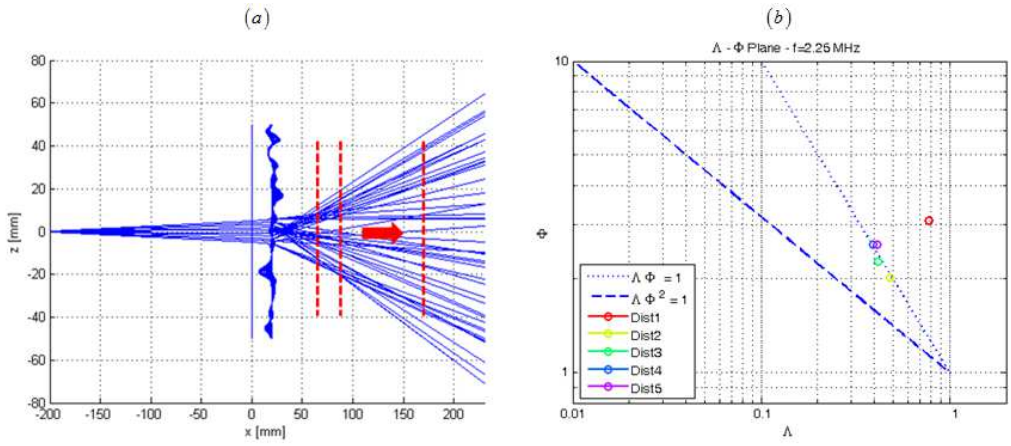

Fig.1: (a): Ray Trace – Vertical Direction – Wax Lens;
(b): ΛΦ Plane – 256 Sensors Vertical Array – f=2.25MHz.

3. EXPERIMENTAL CONFIGURATION.

Our idea is here to develop an experimental configuration that would allow us to observe acoustic signals obtained in the various regimes of saturation defined by Flatté. Thus, the goal of this study is to be able to observe perturbations of the acoustic signals similar to the ones observed in the case of a sound wave propagating through an internal wave field. This translates by distortions and folding of the acoustic wave fronts, and by the presence caustics in the measured pressure field.
The method we adopted for reproducing such phenomena in acoustic tanks is based on the propagation of an ultrasonic signal (f=2.25MHz) through an acoustic lens, and the measurement of the acoustic pressure field propagating through this object and throughout specific regions of the three-dimensional space. A diagram of the experimental configuration is given in Fig.2:

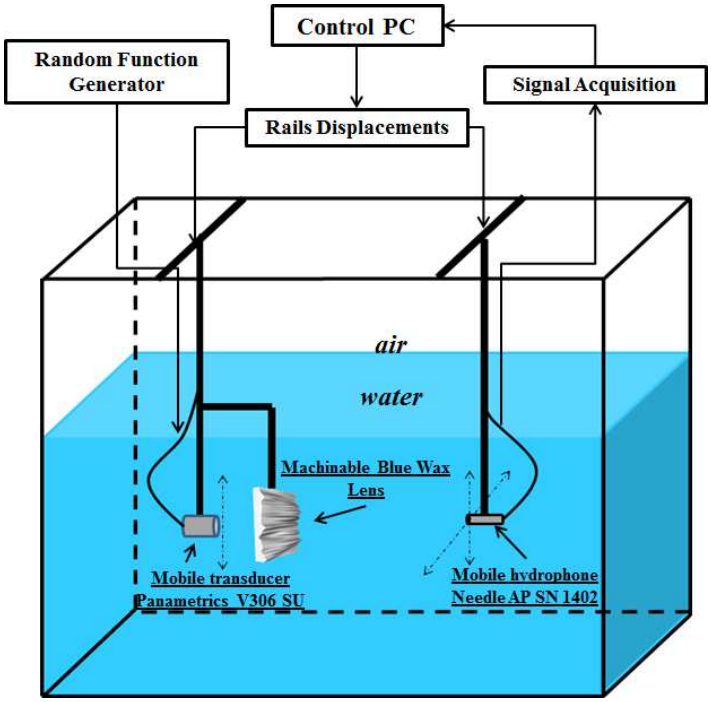

Fig.2: Experimental Configuration Diagram.

The physical properties of the material composing the object are important since they govern the way acoustic rays will be refracted. The material chosen here is referred to as *Machinable Blue Wax* (used in [12]). Its properties are listed in Table 1:

Density	0.98
Longitudinal Wave Sound Speed [m/s]	1975
Shear Wave Sound Speed [m/s]	772
Longitudinal Wave Attenuation [dB/cm]	13 @ 2.25 MHz

Table 1: Physical Properties - Machinable Blue Wax.

It is mainly interesting to notice that the density of the material is very close to the one of water, meaning we can consider the density discontinuity to be quite negligible.
In order for the experimental configuration to match the simulation results, the manufactured distorting object must be as close as possible from the one used in the simulation framework (input plane face and randomly rough output face with

$L_V = 3mm$, $L_H = 30mm$ and $\delta_x = 3mm$) . To do so, we developed a process leading to a sample realized in the appropriate material: first, the profile defined in simulations is interpolated and edited using a CAD software. The output file of the CAD software is then sent to a 3D printer that will produce a first version of the sample.
Nevertheless, the material used by the 3D printer does not feature the appropriate acoustical properties (due to its honeycomb structure), meaning that the printed object will be used as a primary mold to produce the final distorting object in another material. Then, we used a molding silicone (RTV 2-RTV 123) in order to obtain a "negative" mold of the original profile.
This silicone has the advantage to keep its shape at high temperature, and therefore, it allows us to pour the melted *Machinable Blue Wax*. This particular step of the manufacturing process was realized under the dome of an air pumping system in order to avoid the appearance of air bubbles at the surface of the sample.
Fig.3 displays the sample at the different steps of the manufacturing process.

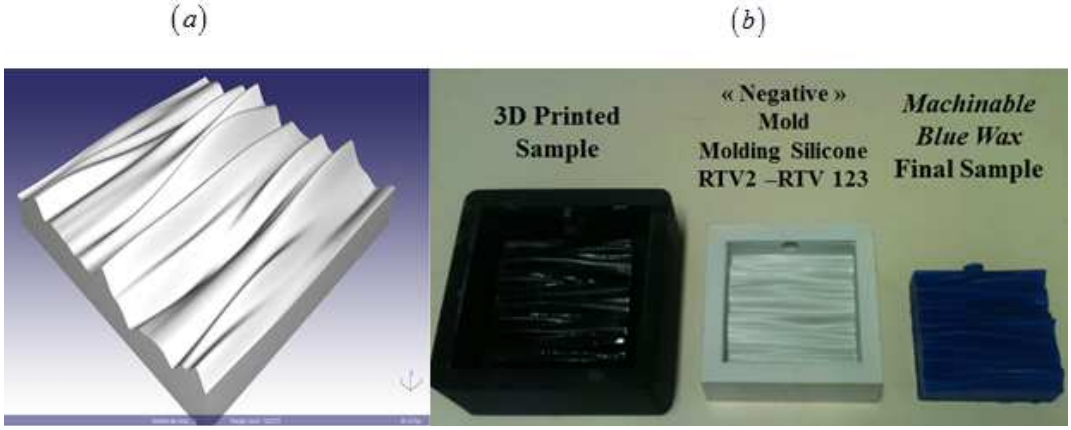

Fig.3: Wax Lens Manufacturing Steps: (a) CAD Software Output; (b) Actual Manufacturing Steps Outputs.

The experimental measurements are conducted in a 3m long, 1.5m wide and 1m deep water. It is filled with fresh water that is controlled using a temperature probe. The acoustic equipment (transducer and hydrophone) as well as the distorting lens are fixed on motorized rails that are driven by a computer interface [13].
The transmitted signal is generated by a random function generator. The signal is then sent through the distorting lens in water using a Panametrics transducer V306-SU, centered at 2.25MHz. The distorted acoustic pressure field is then recorded using a Precision Acoustics Needle Hydrophone. The recording of the sound pressure field is completed at various positions of the hydrophones. The program allowing to control the displacements of the motorized rails also commands automatic interpolated positions, given an initial and a final coordinates and a step size.

4. EXPERIMENTAL RESULTS.

In order to obtain different statistical realizations of the experiment, the depth of the source was changed, so that different regions of the random profiles were acoustically highlighted.

4.1 WAVEFRONT DISTORTIONS.

Fig.4 shows the acoustic envelop of the received signal. This quantity is calculated using the Hilbert transform of the raw received wave train:

$$A_j^e(t) = \log_{10}\left(p_j(t) + iH\left\{p_j(t)\right\}\right), \tag{1}$$

where $p_j(t)$ denotes the acoustic pressure recorded at receiver j and $H\{.\}$ is the Hilbert transform. Distortions are observed when we compare the signal propagated through the wax lens (here at the first distance and center source depth) with the signal propagated in water only. Especially, we notice shadow zones and caustics in the structure of the vertical array wavefront.

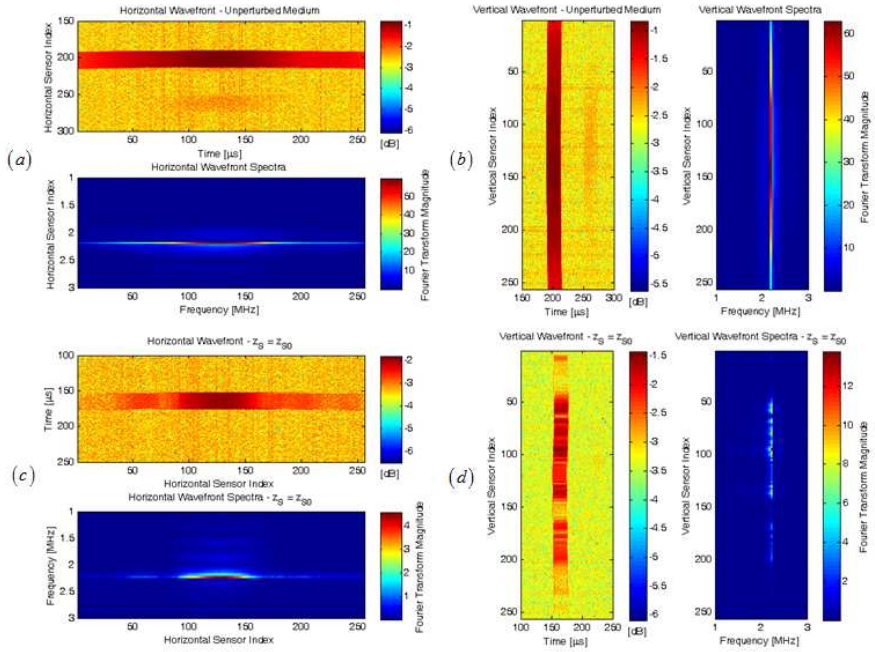

Fig.4: Received Signal Envelop: (a) Unperturbed Medium – Horizontal Array (HA); (b) Unperturbed Medium – Vertical Array (VA); (c) Wax Lens Propagated Signal – HA; (d) Wax Lens Propagated Signal – VA.

4.2 COHERENCE FUNCTION.

We also compared the coherence function calculated with the output of a simulation program presented in [11] with experimental results of the same configuration.

$$C(k\varepsilon) = \left\langle \tilde{p}_l(f_c)\,\tilde{p}_{l+k}{}^*(f_c)\right\rangle_l, \forall l \in [1, N], \forall k \in [1, N-1], \tag{2}$$

Where k is the spacing index, ε represents the spacing between two consecutive sensors, $\tilde{p}_l$ stands for the Fourier transform of the pressure recorded at receiver l , f_c is the signal center frequency and $.^*$ denotes the complex conjugate.

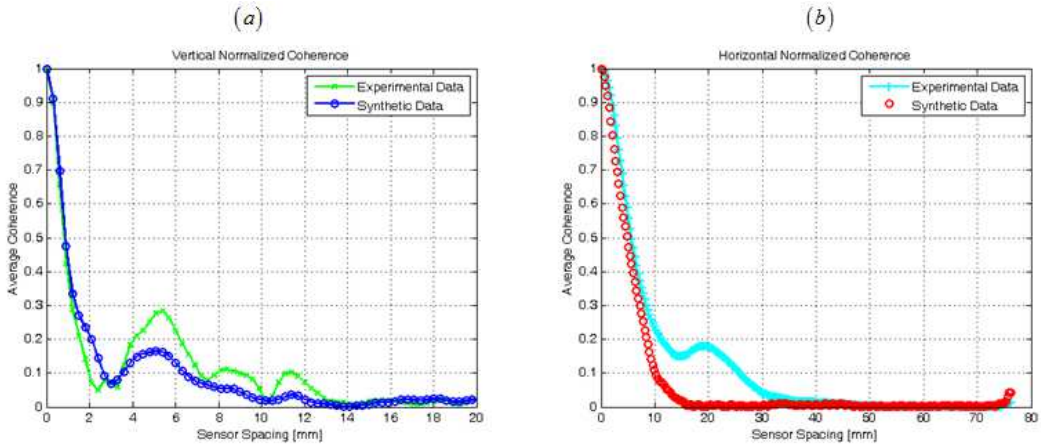

Fig.5: Average Coherence - (a): VA; (b) HA.

Fig.5 displays the average coherence function along the linear array for the first propagation distance ($d_{src/rcvr} = 0.23\ m$).The agreement between the two cases is satisfying for the main lobe, and therefore for the radius of coherence, whose value can be related to the array gain [7]. We observe here a strong degradation of the array performance. Even if the vertical array case displays a decrease of the radius of coherence, the influence of the transducer directivity is noticeable: in the unperturbed medium case, the coherence function is very close to the horizontal array case.

4.3 DETECTION ALGORITHM.

In order to measure the influence of the propagation of acoustic signal through a perturbed medium, we also developed a near-field and range-dependent beam forming routine, i.e. a focalization algorithm.

$$\mathrm{b}(x,y) = 20\log\left[\left|\frac{1}{N}\sum_{l=1}^{N} w_l\, p_l\left(t - \frac{\left|\overrightarrow{MS_l}\right|}{c}\right)\right|\right], \tag{3}$$

where w_l is the weight vector corresponding to sensor l , S_l is the $l-th$ sensor, M is a point of coordinates (x,y) and c is the sound speed in water.

The localization of the source in the case of propagation through an unperturbed medium (Fig.5 (a) and (b)) corresponds to the maximum of the represented function. The position of the source is here obtained with a good precision and matches the experimental configuration. As depicted in Fig.5 (c) and (d), the localization of the source is made more difficult when the focalization algorithm is applied to signals propagated through the wax sample and measured.

If we focus on the vertical antennae case, we observe strong distortions of the focalization output.

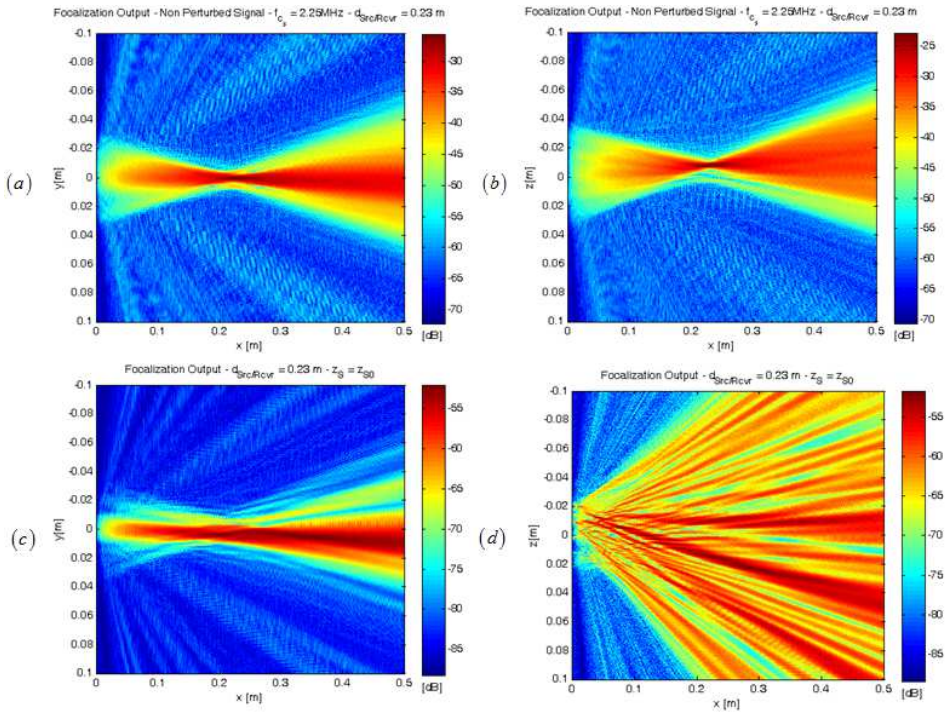

Fig.6: Focalization Algorithm Output: (a) Unperturbed Medium –HA; (b) Unperturbed Medium –VA; (c) Wax Lens Propagated Signal – HA; (d) Wax Lens Propagated Signal – VA.

5. CONCLUSION

In this paper, we presented an experimental protocol allowing us to measure distortions of acoustic signals propagated through a wax lens that we also manufactured. We conducted series of experiment in a controlled environment leading to degradation of linear array performances. We anticipated for the experimental results with ray tracing programs allowing us to classify the signal fluctuations in Flatté's ΛΦ plane. We observed distortions of the signal envelop both for vertical and horizontal linear array and measured the degradation of their detection performances with the calculation of the coherence function. The output of a spherical beam forming algorithm confirmed the fact that the distortion effects prevent the algorithm from accurately detecting the position and direction of the source. Future work will consist in improving the experimental protocol in order to quantitatively scale the distorted acoustic field characteristics (such as the correlation length to wavelength ratio) to the ocean case. Also, signal processing techniques including de-coherence model based optimal filter or beacon based techniques will be tested on both synthetic and experimental data.

ACKNOWLEDGMENT

This work is sponsored by a research grant of the Mission pour la Recherche et l'Innovation Scientifique (DGA – MRIS), the Laboratory of Mechanics and Acoustics (LMA – CNRS) and Thales Underwater Systems.

REFERENCES

[1] I. Newton, "Opticks", Fourth Edition, 1704.
[2] V. I. Tatarskii, "The effects of the Turbulent Atmosphere on Wave Propagation", Keter Press, Jerusalem, 1971.
[3] S. A. Metchev, L. A. Hillenbrand, and R. J. White, "Adaptive optics observations of vega: eight detected sources and upper limits to planetary-mass companions", The Astrophysical Journal, 582(2):1102, 2003.
[4] R. Dashen, W.H. Munk, K.M Watson and F. Zachariasen, "Sound Transmission Through a Fluctuating Ocean", Cambridge University Press, 1979.
[5] S.M. Flatté, "Wave Propagation Through Random Media: Contributions from Ocean Acoustics", Proc. Of the IEEE, 71(11), 1267-1294, 1983.
[6] R. Laval and Y. Labasque, "Medium Inhomogeneities and Instabilities: Effects on Spatial and Temporal Processing", Underwater Acoustics and Signal Processing, 41-70, Springer Netherlands, 1981.
[7] E. Y. Gorodetskaya, A. I. Malekhanov, A. G. Sazontov, and N. K. Vdovicheva, "Deep-water acoustic coherence at long ranges: Theoretical prediction and effects on large-array signal processing", Oceanic Engineering, IEEE Journal of, 24(2):156-171, 1999.
[8] D. Fattaccioli and X. Cristol, "Degradation of Sonar Processing Performances in Random Fluctuating Environments", Proceedings of D. Weston Symposium on Validation of Sonar Performance Assessment Tools, Clare College, Cambridge, UK, 7-9 April 2010.
[9] X. Cristol, D. Fattaccioli and A.S. Couvrat, "Alternative criteria for sonar array-gain limits from linear internal waves", Proceedings of ECUA 2012 (European Conference on Underwater Acoustics), Edimburg, UK, 2-6 July 2012.
[10] D.R. Morgan and T.M. Smith, "Coherence Effects on the Detection Perfomance of Quadratic Array Processors, with Applications to Lage-Array Matched-Field Beamforming", The Journal of the Acoustical Society of America, 87(2), 737-747, 1990.
[11] G. Real, X. Cristol, J.-P. Sessarego, and D. Fattaccioli, "Propagation of Acoustic Waves through A Spatially Fluctuating Medium: Theoretical Study of the Physical Phenomena", Proc. Of the 2nd Underwater Acoustic Conference, Rhodes, GREECE, 23-28 June 2014.
[12] D. C. Calvo, G. C., R. J. Soukup, E.L. Kunz, J.-P. Sessarego, and K. Rudd, " Benchmarking of computational scattering models using underwater acoustic data from a corrugated wax slab", The Journal of the Acoustical Society of America, 123(5): 3602-3602, 2008.
[13] P. Papadakis, M. Taroudakis, F. Sturm, P. Sanchez, and J.-P. Sessarego, "Scaled laboratory experiments of shallow water acoustic propagation: Calibration phase", Acta Acustica united with Acustica, 94(5):676_684, 2008.
[14] G. Real, J.-P. Sessarego, X. Cristol and D. Fattaccioli, "Experimental Study of the Influence of Spatial Inhomogeneities in Underwater Acoustic Propagation", Proc. Of the 1st Underwater Acoustic Conference, Corfu, GREECE, 23-28 June 2013.